

# Enhancing the soft magnetic properties of FeGa with a non-magnetic underlayer for microwave applications

Cite as: Appl. Phys. Lett. **116**, 222404 (2020); <https://doi.org/10.1063/5.0007603>

Submitted: 20 March 2020 . Accepted: 14 May 2020 . Published Online: 02 June 2020

 Adrian Acosta,  Kevin Fitzell,  Joseph D. Schneider,  Cunzheng Dong,  Zhi Yao,  Yuanxun Ethan Wang,  Gregory P. Carman,  Nian X. Sun, and  Jane P. Chang



View Online



Export Citation



CrossMark

## ARTICLES YOU MAY BE INTERESTED IN

[Underlayer effect on the soft magnetic, high frequency, and magnetostrictive properties of FeGa thin films](#)

Journal of Applied Physics **128**, 013903 (2020); <https://doi.org/10.1063/5.0011873>

[Magnetization switching by nanosecond pulse of electric current in thin ferrimagnetic film near compensation temperature](#)

Applied Physics Letters **116**, 222401 (2020); <https://doi.org/10.1063/5.0010687>

[The accurate measurement of spin orbit torque by utilizing the harmonic longitudinal voltage with Wheatstone bridge structure](#)

Applied Physics Letters **116**, 222402 (2020); <https://doi.org/10.1063/1.5145221>



## Your Qubits. Measured.

Meet the next generation of quantum analyzers

- Readout for up to 64 qubits
- Operation at up to 8.5 GHz, mixer-calibration-free
- Signal optimization with minimal latency

[Find out more](#)



# Enhancing the soft magnetic properties of FeGa with a non-magnetic underlayer for microwave applications

Cite as: Appl. Phys. Lett. **116**, 222404 (2020); doi:10.1063/5.0007603

Submitted: 20 March 2020 · Accepted: 14 May 2020 ·

Published Online: 2 June 2020



View Online



Export Citation



CrossMark

Adrian Acosta,<sup>1</sup> Kevin Fitzell,<sup>1</sup> Joseph D. Schneider,<sup>2</sup> Cunzheng Dong,<sup>3</sup> Zhi Yao,<sup>4</sup> Yuanxun Ethan Wang,<sup>4</sup> Gregory P. Carman,<sup>2</sup> Nian X. Sun,<sup>3</sup> and Jane P. Chang<sup>1,a)</sup>

## AFFILIATIONS

<sup>1</sup>Department of Chemical and Biomolecular Engineering, University of California, Los Angeles, California 90095, USA

<sup>2</sup>Department of Mechanical and Aerospace Engineering, University of California, Los Angeles, California 90095, USA

<sup>3</sup>Department of Electrical and Computer Engineering, Northeastern University, Massachusetts 02115, USA

<sup>4</sup>Department of Electrical and Computer Engineering, University of California, Los Angeles, California 90095, USA

<sup>a)</sup>Author to whom correspondence should be addressed: [jpchang@ucla.edu](mailto:jpchang@ucla.edu)

## ABSTRACT

An ultra-thin (~2.5 nm) non-magnetic Cu underlayer was found to have a significant effect on the microstructure, magnetic softness, and magnetostriction of sputter-deposited  $\text{Fe}_{81}\text{Ga}_{19}$  (FeGa) thin films. Compared to the experimental control where FeGa was deposited directly on Si without an underlayer, the presence of Cu increased the in-plane uniaxial anisotropy of FeGa and reduced the in-plane coercivity by nearly a factor of five. The effective Gilbert damping coefficient was also significantly reduced by a factor of four, between FeGa on Si and FeGa on a Cu underlayer. The FeGa films on Cu also retained a high saturation magnetostriction comparable to those without an underlayer. The enhancement of the desirable magnetic properties for microwave applications is attributed to the Cu underlayer, promoting the (110) film texture and increasing the compressive film strain. The results demonstrated that the structural control is viable to simultaneously achieve the necessary magnetic softness and magnetostriction in FeGa for integration in strain-mediated magnetoelectric and microwave devices.

Published under license by AIP Publishing. <https://doi.org/10.1063/5.0007603>

The efficient control of magnetism at the nanoscale via voltage in magnetoelectric (ME) composites has a potential impact in several technologically important areas, such as next-generation memory and logic devices as well as microscale antenna devices.<sup>1–3</sup> One of the major material design challenges in the coupling and efficiency of strain-mediated ME devices is the lack of ferromagnetic materials that exhibit both high magnetostriction and magnetic softness to achieve a high magnetomechanical coupling.

$\text{Fe}_x\text{Ga}_{1-x}$  is a ferromagnetic material that exhibits fairly high magnetostriction in bulk and polycrystalline alloys, which makes it promising for strain-mediated ME devices.<sup>4–8</sup> One of the barriers for high frequency applications of FeGa films has been their large ferromagnetic resonance (FMR) linewidth, which is typically observed in the range of ~620–700 Oe at the X-band for the [100] easy axis.<sup>9,10</sup> However, more recent works have shown that the fabrication of high quality epitaxial films can exhibit greatly enhanced high frequency properties achieving narrower FMR linewidths in the range of ~80–220 Oe at the X-band along the [100] easy axis.<sup>11,12</sup> Indeed, the

deposition parameters can have a significant influence on the structure, magnetic softness, and magnetostrictive properties of FeGa thin films and have been well documented.<sup>13–17</sup> Along that line, researchers have also explored the addition of C, B, and N to FeGa thin films to promote soft magnetic properties by reducing their grain size and diminishing their magnetocrystalline anisotropy.<sup>4,18,19</sup>

A number of studies have previously explored the effect of underlayers (such as Ru, NiFe, Cu, Co, etc.) between the substrate and sputtered FeCo thin films on their soft magnetic properties.<sup>20–27</sup> The observed enhancement in the soft magnetic properties of FeCo has been attributed to the effect of the underlayer on the interfacial magnetoelastic energy.<sup>20,28–30</sup> Similarly, in this work, the strategy of using a non-magnetic underlayer (Cu) was explored to study its effect on the microstructure and texture of the FeGa film, which dictates the attainable magnetic softness and magnetostriction.

The FeGa and Cu films in this study were grown via DC magnetron sputter deposition using an ULVAC JSP 8000 sputter system with a base pressure of  $2 \times 10^{-7}$  Torr at room temperature. Si (100)

substrates were used for all the depositions without any initial removal of the native oxide. The FeGa films were formed using a target with an Fe to Ga ratio of 80/20 at a DC bias power of 200 W and an Ar pressure of 0.5 mTorr; the Cu underlayer was sputtered at a DC bias power of 100 W and an Ar pressure of 0.5 mTorr. Scanning electron microscopy (SEM) imaging was used to calibrate the growth rate of the films. The thickness of the FeGa films was measured to be  $100.3 \pm 1.7$  nm (see Fig. S1); the nominal value is henceforth referred to as 100 nm. The relative composition of the FeGa films was measured at Fe:Ga ( $81.4 \pm 3.0$ ):( $18.6 \pm 0.5$ ), which was determined via x-ray photoelectron spectroscopy (XPS) with a mono-chromated Al K $\alpha$  source (see Fig. S2). The structures of the films were characterized via x-ray diffraction (XRD) using a Panalytical X'Pert Pro X-ray Powder Diffractometer with a Cu K $\alpha$  source and Fityk software package.<sup>31</sup>

The room temperature magnetic properties of FeGa thin films were measured via superconducting quantum interference device (SQUID) magnetometry using a Quantum Design MPMS3. The high-frequency FMR linewidth was measured using a short-circuited strip line connected to a vector network analyzer (VNA). For these measurements, the samples were placed facing the strip line and a large saturating magnetic field was first applied parallel to the strip line to establish a baseline for the measurement. The reflection coefficient ( $S_{11}$ ) was then measured as a function of bias magnetic field (0–600 Oe) and frequency (100 MHz to 6 GHz).<sup>32</sup>

Magnetostrictive characterization was performed by depositing FeGa, with and without a Cu underlayer, on thin Si cantilevers (100  $\mu$ m thickness). An MTI-2000 fiber-optic sensor was used to detect the deflection of the cantilever tip due to changes in the internal stress of the FeGa thin films, with details described elsewhere.<sup>18</sup>

In this work, thin films of  $\text{Fe}_{81}\text{Ga}_{19}$  (100 nm) were deposited either directly onto Si substrates or with a thin 2.5 nm Cu underlayer. Figure 1 shows the in-plane magnetic hysteresis (MH) loops for the 100 nm FeGa films deposited on Si with and without a Cu underlayer normalized to the saturation magnetization (see Fig. S3 for the full MH loops at high fields). The FeGa film deposited directly onto a Si

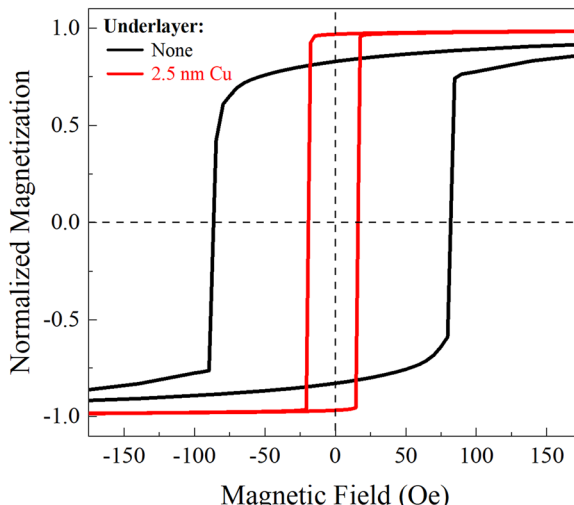


FIG. 1. In-plane magnetic hysteresis loops of 100 nm FeGa sputtered on a Si substrate with and without a Cu underlayer.

substrate, without the Cu underlayer, shows a coercivity of 84 Oe. For an FeGa film deposited onto a 2.5 nm Cu underlayer, a much smaller coercivity of 17 Oe was achieved. These results are consistent with those previously observed for FeCo films in which a Cu underlayer promotes a large decrease in in-plane coercivity.<sup>20,24,33</sup> Additionally, the FeGa films deposited with a Cu underlayer displayed an enhanced uniaxial anisotropy, as observed from the increase in remnant magnetization.

The high-frequency characteristics of FeGa films deposited on Si with and without a Cu underlayer were studied using broadband FMR spectroscopy. Figure 2 shows the  $S_{11}$  absorption as a function of magnetic bias field (0–600 Oe) at a fixed frequency of 6 GHz. These  $S_{11}$  absorption spectra are cross sections of the entire FMR spectra over the frequency range of 100 MHz–6 GHz (inset).

For a 100 nm FeGa film deposited without an underlayer, the FMR spectra are characterized by a very low peak absorption and very broad FMR linewidth (>600 Oe at 6 GHz) that extends beyond the maximum magnetic field applied. In contrast, the FeGa film deposited on a Cu underlayer is characterized by a significant enhancement in the FMR response with a narrow linewidth of  $\sim 190$  Oe at 6 GHz.

The effective Gilbert damping coefficient,  $\alpha_{\text{eff}}$ , was calculated by fitting the FMR linewidth of the absorption as a function of frequency for the FMR spectra from 3 GHz to 6 GHz to the equation:  $\Delta H = 2\alpha_{\text{eff}}\omega/\gamma + \Delta H_0$ , where  $\omega$  is the frequency,  $\gamma$  is the gyromagnetic ratio ( $\approx 2.8$  MHz/Oe), and  $\Delta H_0$  is the frequency-independent linewidth broadening (see Fig. S4). The value of  $\alpha_{\text{eff}}$  for FeGa on Si was  $0.21 \pm 0.11$  but decreased to  $0.05 \pm 0.01$  when grown with a Cu underlayer.

The enhanced soft magnetic properties of the FeGa film grown on an underlayer originated from the effect of the underlayer on its microstructure. Structural characterization of the FeGa films was first

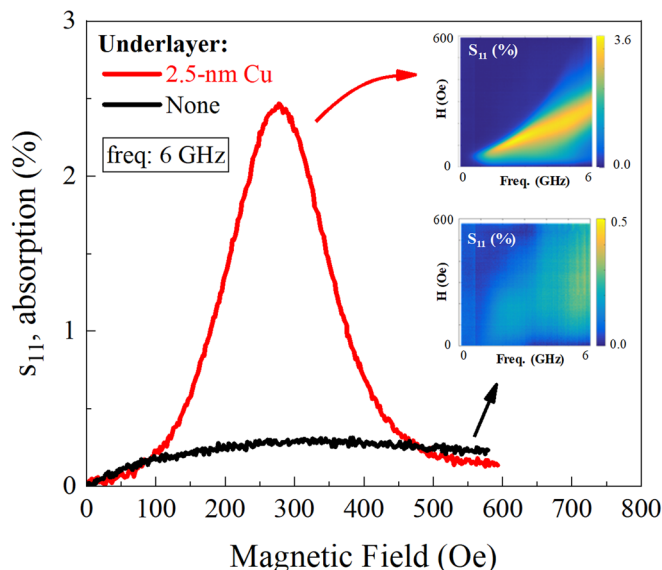


FIG. 2.  $S_{11}$  absorption spectra as a function of magnetic bias field at 6 GHz for 100 nm FeGa films sputtered with and without a Cu underlayer. The insets show FMR spectra as a function of both frequency (100 MHz–6 GHz) and magnetic bias (0–600 Oe).

investigated using XRD. Figure 3 shows the spectra highlighting the bcc (110) diffraction for a 100 nm FeGa film sputtered with and without a Cu underlayer. The films deposited onto a Cu underlayer display a large shift of the (110) diffraction line position, which is caused by relative changes in the strain of the films. The shift in the peak position represents a relative increase of 0.28% compressive strain for the FeGa film on Cu compared to FeGa deposited directly onto a Si substrate.

The FeGa film deposited with a Cu underlayer also showed an increase (~30%) in the intensity of the (110) diffraction peak as compared to that without an underlayer, indicating an increased (110) polycrystalline texture. This enhancement can be attributed to the close lattice match of the FeGa (110) film texture ( $d = 2.058 \pm 0.001 \text{ \AA}$ ) during growth to the underlying Cu (111) film texture ( $d = 2.087 \pm 0.001 \text{ \AA}$ ), which is highlighted in supplemental Fig. S5. This is consistent with a previous study that used Cu as a buffer layer to achieve epitaxial growth of FeGa films by encouraging a (110) crystalline texture along the growth direction.<sup>34</sup> However, a broader comparison of the impact of Cu as a buffer layer for sputtered FeGa films on their soft magnetic and magnetostrictive properties has not been studied, which is the focus of this work. Furthermore, it is expected that there is a reduction in the grain width for the FeGa films with a Cu underlayer (evidenced by the underlayer studies for FeCo films<sup>20,25–27</sup>); however, while the trends in the full-width at half-maximum of the peaks can generally provide insight into the grain size, the XRD data only capture the lattice spacing for out-of-plane diffraction and would not be appropriate for examining changes in the width of the grains that would be in-plane to the film.

In order to obtain magnetostriction measurements for FeGa films, a perpendicular AC magnetic field is applied along the short axis of the silicon cantilever during the measurement, while a 100 Oe bias field is initially applied and held constant in the long axis in order to saturate the magnetization and assess the full magnetostriction. The magnetic field-induced stress,  $b$ , is calculated from the deflection at the cantilever tip using the following relation from Ref. 35:  $b = -dt_s^2 E_s / 3t_f l^2 (1 + \nu_s)$ ,

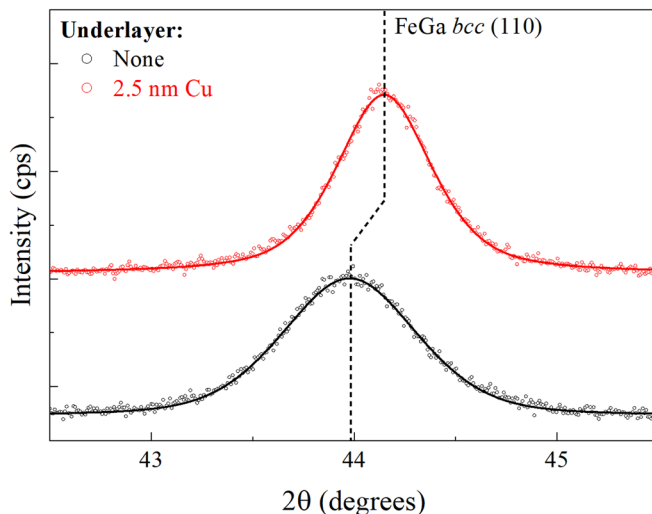


FIG. 3. XRD spectra of the main bcc (110) FeGa peak when grown with and without a Cu underlayer. Solid lines are the best voigt fit of the data in circles. Vertical dashed lines are used to highlight the shift in the (110) peak across samples.

where  $d$  is the deflection,  $t_s$  and  $t_f$  are the substrate and film thicknesses (100  $\mu\text{m}$  and 100 nm, respectively),  $l$  is the distance between the clamping edge and the probe location (27 mm), and  $E_s$  and  $\nu_s$  are the Young's modulus and Poisson ratio of the Si substrate (169 GPa and 0.069, respectively, along the [110] in-plane direction for a Si (100) substrate<sup>36</sup>). Note that the elastic properties of the Cu underlayer are neglected from the calculation as the behavior of the underlayer is dominated by the bulk of the Si substrate.

For thin films, the magnetic field-induced stress is considered the more relevant parameter to describe magnetostrictive effects since the lateral deformation is blocked by the substrate, and one can measure only the stress. This also avoids the need to measure the elastic properties of thin films, which can be difficult. For comparison to other literature studies on magnetostrictive thin films, the magnetostriction in terms of strain can be assessed from the relation of  $\lambda = -\frac{2}{3} \left( \frac{1+\nu_f}{E_f} \right) \times b$ , where  $E_f$  and  $\nu_f$  are the Young's modulus and Poisson ratio of the FeGa film, which are approximated following the convention that  $\left( \frac{E_f}{1+\nu_f} \right) = 50 \text{ GPa}$ .<sup>37</sup>

From the data in Fig. 4, it is found that the FeGa film deposited without an underlayer reaches a maximum magnetic field-induced stress of 7.4 MPa, corresponding to a magnetostriction of 99 ppm. The film grown on the Cu underlayer largely maintains a comparable level of magnetostriction (95 ppm), displaying a maximum magnetic field-induced stress of 7.2 MPa. The importance of the results here is to highlight that the soft magnetic properties of the FeGa films can be enhanced without trade-off of the high magnetostriction values.

In summary, in order to enhance the soft magnetic properties of sputtered FeGa thin films, a strategy of using a thin 2.5 nm Cu underlayer between FeGa and the Si substrate was explored. It was found that an 80% decrease in coercivity and a 75% decrease in the effective Gilbert damping coefficient can be achieved by using Cu as an underlayer. It is observed that an underlayer serves to influence the

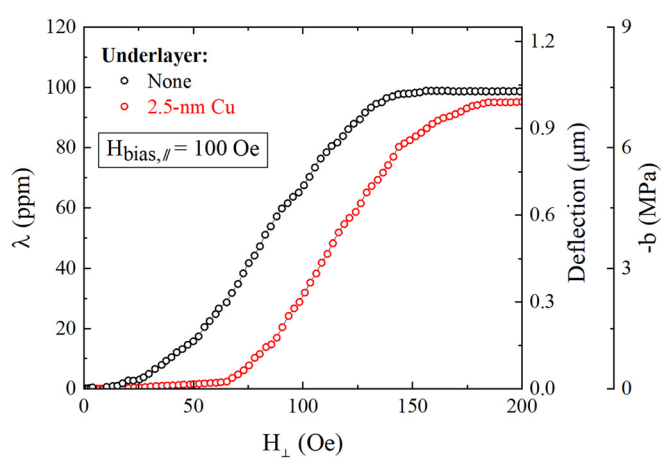


FIG. 4. (Left axis): calculated magnetostriction for 100 nm FeGa sputtered with and without a Cu underlayer as a function of the AC magnetic field (along the short axis of the cantilever sample). (Right axes): directly measured cantilever deflection and corresponding calculated stress. An initial bias field of 100 Oe was applied to saturate the magnetization along the long axis of the cantilever sample and held constant during the measurement.

microstructure of the FeGa films, resulting in an increased (110) polycrystalline texture and an increase in compressive film strain for the FeGa films. The saturation magnetostriction is largely retained for an FeGa film grown with a Cu underlayer (95 ppm) compared to the FeGa film without an underlayer (99 ppm).

These results demonstrate that the underlayer strategy is effective at providing structural control to simultaneously enhance the magnetic softness of FeGa while retaining its desirable magnetostrictive properties. High magnetostriction, low effective Gilbert damping, and low coercivity of FeGa grown on a lattice-matched underlayer such as Cu make it an attractive material for strain-mediated ME and other microwave device applications.

See the [supplementary material](#) for SEM imaging, XPS scans, full scale in-plane MH loops for the FeGa films, and complete XRD spectra of FeGa, Cu, and Si substrate materials.

We acknowledge the use of the fabrication facility at the Integrated Systems Nanofabrication Cleanroom (ISNC) and the Molecular Instrumentation Center (MIC) at the California NanoSystems Institute (CNSI) at UCLA. This work was also supported by the NSF Nanosystems Engineering Research Center for Translational Applications of Nanoscale Multiferroic Systems (TANMS) under the Cooperative Agreement Award (No. EEC-1160504). Ryan Sheil is acknowledged for performing the XRD and XPS measurements.

## DATA AVAILABILITY

The data that support the findings of this study are available from the corresponding author upon reasonable request.

## REFERENCES

- <sup>1</sup>K. Roy, S. Bandyopadhyay, and J. Atulasimha, *Appl. Phys. Lett.* **99**(6), 063108 (2011).
- <sup>2</sup>C. Song, B. Cui, F. Li, X. Zhou, and F. Pan, *Prog. Mater. Sci.* **87**, 33 (2017).
- <sup>3</sup>T. Nan, H. Lin, Y. Gao, A. Matyushov, G. Yu, H. Chen, N. Sun, S. Wei, Z. Wang, M. Li, X. Wang, A. Belkessam, R. Guo, B. Chen, J. Zhou, Z. Qian, Y. Hui, M. Rinaldi, M. E. McConney, B. M. Howe, Z. Hu, J. G. Jones, G. J. Brown, and N. X. Sun, *Nat. Commun.* **8**(1), 296 (2017).
- <sup>4</sup>D. Cao, X. Cheng, L. Pan, H. Feng, C. Zhao, Z. Zhu, Q. Li, J. Xu, S. Li, and Q. Liu, *AIP Adv.* **7**(11), 115009 (2017).
- <sup>5</sup>A. E. Clark, M. Wun-Fogle, J. B. Restorff, and T. A. Lograsso, *Mater. Trans.* **43**(5), 881 (2002).
- <sup>6</sup>N. Srisukhumbowornchai and S. Guruswamy, *J. Appl. Phys.* **90**(11), 5680 (2001).
- <sup>7</sup>W. Jahjah, J.-P. Jay, Y. Le Grand, A. Fessant, A. R. E. Prinsloo, C. J. Sheppard, D. T. Dekadjevi, and D. Spenato, *Phys. Rev. Appl.* **13**(2), 034015 (2020).
- <sup>8</sup>M. J. Jiménez, G. Cabeza, J. E. Gómez, D. Velázquez Rodriguez, L. Leiva, J. Milano, and A. Butera, *J. Magn. Magn. Mater.* **501**, 166361 (2020).
- <sup>9</sup>A. Butera, J. Gómez, J. L. Weston, and J. A. Barnard, *J. Appl. Phys.* **98**(3), 033901 (2005).
- <sup>10</sup>J. Lou, R. E. Insignares, Z. Cai, K. S. Ziemer, M. Liu, and N. X. Sun, *Appl. Phys. Lett.* **91**(18), 182504 (2007).
- <sup>11</sup>D. E. Parkes, L. R. Shelford, P. Wadley, V. Holý, M. Wang, A. T. Hindmarch, G. Van Der Laan, R. P. Campion, K. W. Edmonds, and S. A. Cavill, *Sci. Rep.* **3**, 2220 (2013).
- <sup>12</sup>S. Budhathoki, A. Sapkota, K. M. Law, B. Nepal, S. Ranjit, K. C. Shambhu, T. Mewes, and A. J. Hauser, *J. Magn. Magn. Mater.* **496**, 165906 (2020).
- <sup>13</sup>A. Javed, N. A. Morley, and M. R. J. Gibbs, *J. Magn. Magn. Mater.* **321**(18), 2877 (2009).
- <sup>14</sup>A. Javed, N. A. Morley, and M. R. J. Gibbs, *J. Appl. Phys.* **107**(9), 09A944 (2010).
- <sup>15</sup>A. Javed, T. Szumiata, N. A. Morley, and M. R. J. Gibbs, *Acta Mater.* **58**(11), 4003 (2010).
- <sup>16</sup>H. Basumatary, J. Arout Chelvane, D. V. Sridhara Rao, S. V. Kamat, and R. Ranjan, *J. Magn. Magn. Mater.* **384**, 58 (2015).
- <sup>17</sup>E. C. Estrine, W. P. Robbins, M. M. Maqableh, and B. J. Stadler, *J. Appl. Phys.* **113**(17), 17A937 (2013).
- <sup>18</sup>C. Dong, M. Li, X. Liang, H. Chen, H. Zhou, X. Wang, Y. Gao, M. E. McConney, J. G. Jones, and G. J. Brown, *Appl. Phys. Lett.* **113**(26), 262401 (2018).
- <sup>19</sup>X. Liang, C. Dong, S. J. Celestin, X. Wang, H. Chen, K. S. Ziemer, M. Page, M. E. McConney, J. G. Jones, and B. M. Howe, *IEEE Magn. Lett.* **10**, 1 (2019).
- <sup>20</sup>H. S. Jung, W. D. Doyle, and S. Matsunuma, *J. Appl. Phys.* **93**(10), 6462 (2003).
- <sup>21</sup>Y. Fu, X. Cheng, and Z. Yang, *Phys. Status Solidi A* **203**(5), 963 (2006).
- <sup>22</sup>X. Liu, H. Kanda, and A. Morisako, *J. Phys.: Conf. Ser.* **266**, 012037 (2011).
- <sup>23</sup>Y. Li, Z. Li, X. Liu, Y. Fu, F. Wei, A. S. Kamzin, and D. Wei, *J. Appl. Phys.* **107**(9), 09A325 (2010).
- <sup>24</sup>H. S. Jung, W. D. Doyle, J. E. Wittig, J. F. Al-Sharab, and J. Bentley, *Appl. Phys. Lett.* **81**(13), 2415 (2002).
- <sup>25</sup>X. Liu, T. Miyao, Y. Fu, and A. Morisako, *J. Magn. Magn. Mater.* **303**(2), e201 (2006).
- <sup>26</sup>S. Akansel, V. A. Venugopal, A. Kumar, R. Gupta, R. Brucas, S. George, A. Neagu, C.-W. Tai, M. Gubbins, and G. Andersson, *J. Phys. D: Appl. Phys.* **51**(30), 305001 (2018).
- <sup>27</sup>Y. P. Wu, G.-C. Han, and L. B. Kong, *J. Magn. Magn. Mater.* **322**(21), 3223 (2010).
- <sup>28</sup>M. T. Kief, V. Inturi, M. Benakli, I. Tabakovic, M. Sun, O. Heinonen, S. Riemer, and V. Vas'ko, *IEEE Trans. Magn.* **44**(1), 113 (2008).
- <sup>29</sup>H. Xie, K. Zhang, H. Li, Y. Wang, Z. Li, Y. Wang, J. Cao, J. Bai, F. Wei, and D. Wei, *IEEE Trans. Magn.* **48**(11), 2917 (2012).
- <sup>30</sup>L. Cabral, F. H. Aragón, L. Villegas-Lelovsky, M. P. Lima, W. A. A. Macedo, and J. L. Da Silva, *ACS Appl. Mater. Interfaces* **11**(1), 1529 (2019).
- <sup>31</sup>M. Wojdry, *J. Appl. Crystallogr.* **43**(5), 1126 (2010).
- <sup>32</sup>W. G. Q. Xu and Y. E. Wang, “Two dimensional (2D) complex permeability characterization of thin film ferromagnetic material,” in *2016 IEEE Conference on Antenna Measurements & Applications (CAMA), Syracuse, NY, 23-27 Oct. 2016* (IEEE, 2017), pp. 1–4.
- <sup>33</sup>S. Cakmaktepe, M. I. Coskun, and A. Yildiz, *Lith. J. Phys.* **53**(2), 112 (2013).
- <sup>34</sup>J. L. Weston, A. Butera, T. Lograsso, M. Shamsuzzoha, I. Zana, G. Zangari, and J. Barnard, *IEEE Trans. Magn.* **38**(5), 2832 (2002).
- <sup>35</sup>E. du Trémolet De Lacheisserie and J. C. Peuzin, *J. Magn. Magn. Mater.* **136**(1–2), 189 (1994).
- <sup>36</sup>M. A. Hopcroft, W. D. Nix, and T. W. Kenny, *J. Microelectromech. Syst.* **19**(2), 229 (2010).
- <sup>37</sup>J. R. Hattrick-Simpers, D. Hunter, C. M. Craciunescu, K. S. Jang, M. Murakami, J. Cullen, M. Wuttig, I. Takeuchi, S. E. Lofland, and L. Benderksy, *Appl. Phys. Lett.* **93**(10), 102507 (2008).